IL NUOVO CIMENTO **41 C** (2018) 117
DOI 10.1393/ncc/i2018-18117-5

COMMUNICATIONS: SIF Congress 2017

Simulations and test beam studies of the iMPACT calorimeter

F. BARUFFALDI(*)

Dipartimento di Fisica e Astronomia, Università di Padova - Padova, Italy

received 31 January 2018

Summary. — This contribution describes the first results obtained within the iMPACT project, which aims to build a novel proton computed tomography (pCT) scanner for protons of energy up to 230 MeV, as used in hadron therapy. We will first describe the design of the iMPACT scanner, which is composed by a tracker and a range calorimeter. Results of test-beams, focused on the characterization of the building elements of the prototype of the calorimeter, will be presented and compared with simulations.

1. – Introduction

Hadron therapy is a leading-edge technique which exploits the particular energy deposition profile (Bragg peak) that protons or heavy ions exhibit to target and destroy tumors within the human body. The beneficial aspects of this technique over other, more established, procedures, such as X-ray therapy, have been extensively reported [1].

The effectiveness of a hadron therapy treatment relies on the knowledge of the tissues density or, equivalently, the stopping power (SP) distribution: an accurate 3D map of the body SP is necessary to precisely determine the position of the Bragg peak as a function of the beam energy. The effectiveness of the hadron therapy procedure is currently limited by the necessity to rely on body density maps produced with X-ray Computed Tomography (X-ray CT), which cannot deliver maps accurate enough to fully exploit the intrinsic accuracy of the technique [2]. This is mainly due to the different behaviour inside matter of X-ray and hadrons. The proton beam range prediction, obtained from CT, can be affected by uncertainties up to 3 mm [3]. It is worth mentioning that more recently developed X-ray CT tecniques, such as dual-energy CT (DECT), have shown the potential to lower the range uncertainties by 0.6–1.1 mm with respect to the standard CT [3].

(*) E-mail: filippo.baruffaldi@studenti.unipd.it

A Computed Tomography performed with protons (pCT), instead of X-ray, would further improve the accuracy of the SP maps and lead to an enhancement of the treatment effectiveness, as the particles used for both the imaging process and the treatment present the same energy loss behaviour. Studies confirmed that pCT can potentially lower the proton range uncertainties to approximately 1 mm [4]. In addition, the dose delivered to the patient with a pCT is limited to few mGy, at least an order of magnitude lower than the dose delivered with a traditional X-ray CT (10–100 mGy) [2, 5]. However, the spatial resolution is expected to be worse for pCT than X-ray CT, mostly due to protons multiple Coulomb scattering (MCS) [6].

The iMPACT Project, *innovative Medical Proton Achromatic Calorimeter and Tracker*, aims to design and develop a pCT scanner, with the ultimate goal of demonstrating the viability of the pCT technique in a realistic clinical environment.

2. – Proton computed tomography

Nowadays several pCT scanner prototypes are being studied around the world [7]. All the existing setups share very similar layouts, featuring two tracking stages, one placed before and one after the scanned object, to measure the position of each entering and exiting proton. The tracking system is coupled with a proton residual energy detector, in order to estimate the energy loss each proton underwent inside the target. Different algorithms and softwares have been developed for the object 3D image reconstruction from the tracks-energy information. Most of these algorithms are based on the Most Likelihood Path (MLP) formalism, which uses the initial and final proton directions to evaluate the most probable proton path inside the object [8]. In a volume of $10 \times 10 \times 10\,\mathrm{cm}^3$ a number of about 10^9 fully measured proton tracks are required to reconstruct a 3D image with the necessary resolution (spatial resolution better than 1 mm, energy resolution better than 1%) [9].

The major limitation preventing pCT to be a viable alternative to X-ray CT is given by the slow acquisition rate that all the existing scanner prototypes feature. With the best present setup, which reaches less than a 10 MHz acquisition rate [7], a complete record of the required number of protons would take several minutes to be completed. With such long scanning times, the image quality becomes affected by motion of internal organs, mainly due to the patient's breathing. Additionally, a clinically viable pCT scanner should sustain the high flux that commercial proton therapy machines provide, usually between 10^6–10^9 particles/s [10].

3. – The iMPACT project

iMPACT is a project started in 2016, funded by an ERC Consolidator Grant (649031). The aim of the project is to develop a clinically viable pCT scanner, capable to record 10^9 proton events in less than 10 s. In order to meet such ambitious requirements, iMPACT plans to exploit cutting-edge technologies under development for particle physics detectors. The system is planned to be realised using commercially available solutions, to reduce material costs and ensure scalability. The iMPACT scanner layout, shown in fig. 1, consists of 4 monolithic active silicon pixel (MAPS) sensors tracking planes, and a highly segmented range calorimeter. The performances of both the tracker and the calorimeter are currently being studied separately, in order to identify the best design choices before combining them into a single instrument that correlates the information of these two separate units.

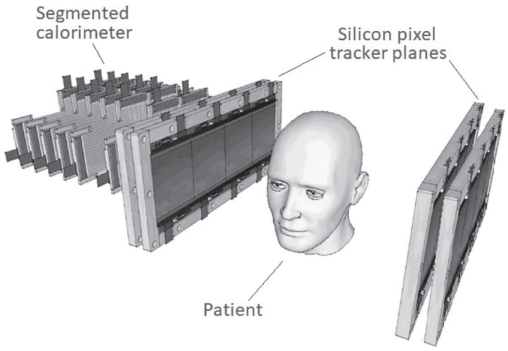

Fig. 1. – Rendering of the iMPACT project scanner layout.

3˙1. *The iMPACT Tracking System.* – Several pixel sensors are being considered for the iMPACT tracker; a pixel sensor design was preferred over other solutions, such as silicon strips, for its intrinsic better performances, in particular higher acquisition rate capability and lower material budget. The ALPIDE sensor, developed within the ALICE Collaboration at the CERN Large Hadron Collider for the Inner Tracking System upgrade, is currently adopted in the iMPACT prototyping phase while more advanced designs are still under development. The ALPIDE sensor, is a 100 μm thick 1.5 cm $\times$ 3 cm large MAPS featuring 28 μm$\times$ 28 μm pixels arranged in a 512 $\times$ 1024 matrix [11]. The chip is produced exploiting commercially available CMOS processes with a monolithic design, *i.e.* the read-out electronics is embedded within the sensor itself, to reduce costs and material budget. A zero-suppression logic is implemented to improve read-out speed and reduce output data volume. The sensor is able to cope with a 100 kHz/cm^2 particle rate. ALPIDE reaches a sub-pixel spatial resolution around 4.6 μm.

3˙2. *The iMPACT range calorimeter.* – The iMPACT scanner includes, together with the tracker system, a scintillator range calorimeter. The calorimeter, outlined in fig. 2, is segmented in the z direction into 5 mm thick plastic scintillator planes with about $40 \times 40\,\mathrm{cm}^2$ surface area, able to scan an object approximately as large as $33 \times 33\,\mathrm{cm}^2$. A total of about 60 planes is foreseen, to completely stop a proton beam up to ~ 200 MeV, the typical hadron therapy energy range. Each plane is further divided, in the x and y directions alternatively, into smaller segments, also referred to as *fingers*, each one 1 cm wide and 20 cm long. The high level of segmentation in the x-y plane allows a

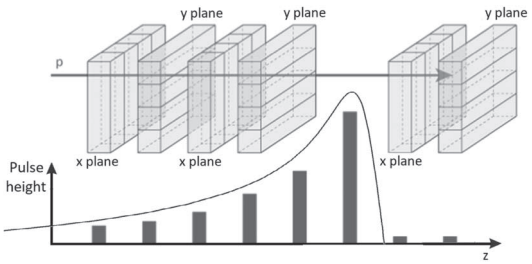

Fig. 2. – iMPACT calorimeter layout, segmented in alternate x and y planes. Vertical bars represent the expected signal amplitudes along the planes.

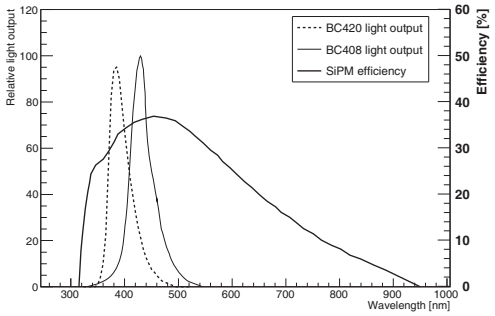

Fig. 3. – Scintillators (BC-420 and BC-408) light output as a function of the wavelength (left axis) compared to SiPM detection efficiency (right axis).

higher detection rate capability of the scanner. Each scintillating finger is independently read-out with a Silicon Photo Multiplier (SiPM). The Hamamatsu S12572-025c SiPMs, with 3 mm × 3 mm active area, were chosen for the calorimeter realization, due to their competitive technical features and the fact that they come in a ceramic mounting package which greatly helps system integration. Each finger is wrapped with a thin, highly reflective teflon layer, to improve light collection, and further shielded by an aluminum layer.

The proton stopping position is estimated observing the depth of the last hit-plane, with an uncertainty of about 1.4 mm (the z-direction segmentation pitch, 5 mm, divided by $\sqrt{12}$). Furthermore, the output signal amplitudes along the planes can be used to reconstruct the shape of the proton Bragg curve, which can then be fitted in order to improve the proton stopping position estimation: thanks to this feature the iMPACT calorimeter can be considered a hybrid *energy range* calorimeter. In this case the proton stopping position can be determined with a sub z-pitch precision between 1.1 and 1.4 mm. Detailed calculations on the stopping position precision achievable with the current setup can be found in [12].

Two different polyvinyl toluene (PVT) scintillators are being taken into consideration: the BC-420, slightly faster, and the BC-408, with emission wavelengths better matched by the SiPM efficiency (fig. 3).

Considering the extremely high number of output channels in the complete calorimeter (more than 2000), an analog readout at hundreds of MHz would be quite impractical, power consuming and expensive. A threshold-based digital discriminator was therefore designed, with the analog SiPM output signals sampled at a number of different amplitude levels (less than 5) by fast comparators. This system is comparable to a 2 or 3 bit ADC. The number and the level of the thresholds are to be optimized from both simulations and experimental data.

4. – Simulations of the basic unit of the iMPACT calorimeter

A Monte Carlo simulation of the calorimeter has been developed in order to evaluate its performance. In the first phase the simulation has been used to optimize the detector constructive parameters; in a more advanced stage, the simulation will also provide experimental-like output data for testing the read-out chain, the data analysis software, and the image reconstruction techniques. The simulation was modelled using the GATE

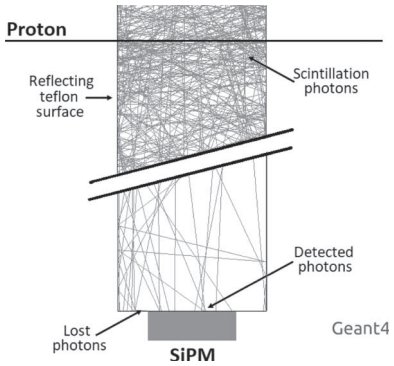

Fig. 4. – Simulated optical photons produced via scintillation inside a PVT finger, photons transportation and different surface properties. The number of generated photons has purposely been reduced by a factor ~ 1000, to help visualizing single photon tracks.

application, an advanced opensource software dedicated to numerical simulations in medical imaging and radiotherapy, based on the Geant4 toolkit [13].

The simulation studies have been initially focused on the characterization and modelling of the scintillation process and the detection of photons in a single PVT finger, which represents the basic unit of the iMPACT calorimeter, as shown in fig. 4. Each scintillation photon, produced by the proton energy deposition, is individually transported through the material; the different surfaces properties, as the finger teflon wrapping, have been defined, in order to simulate a realistic optical behaviour of photons. The SiPM surface in contact with the finger constitutes the primary detector: photons transmitted in the SiPM silicon volume are recorded.

4˙1. *Simulation of the output analog signal.* – The information on each photon detection time, obtained from the Monte Carlo, is used to simulate the experimental analog signal. The SiPM active surface is formed by a matrix of Geiger-mode Avalanche PhotoDiodes (APD) connected in parallel; each of these APD produces an identical pulse when a photon is detected, so a multiple-photon signal is in first approximation given by the pile-up of multiple identical single-photon voltage pulses. An analog simulated signal can therefore be built by summing the same single-photon response for each detected photon, with the starting time of each single-photon pulse given by the simulated photon detection time. The single-photon pulse, generated by an APD on the SiPM surface and shaped by the read-out electronics, has been experimentally sampled, using the apparatus shown in fig. 5 (left). The setup consisted of a pulsed LED diode emitting short (a few ns) and low intensity light pulses toward a reflective teflon surface; the back-diffused photons were detected by a SiPM. The entire apparatus was enclosed in a sealed dark chamber, to isolate the instruments from external light sources. Direct measurements of such a low intensity light source allow to distinguish the contribution of single photons. In fact, the signal amplitude spectrum, displayed in fig. 5 (right), presents equally spaced peaks, where each peak was associated to events with a discrete number of simultaneous detected photons N. The average single-photon signal was finally obtained by averaging the few-photons signals, normalized by their respective N.

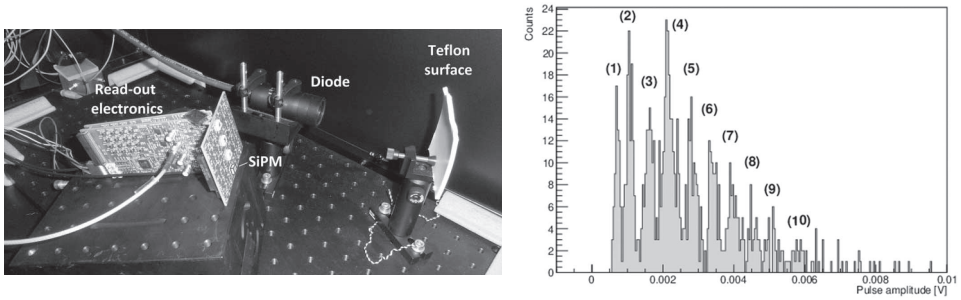

Fig. 5. – Experimental setup for the single photon response measurement (left). Few-photons pulse amplitude spectrum (right). The discrete nature of the pulses is visible, with each peak associated to a countable number of simultaneous detected photons.

5. – Characterization with low energy protons

Preliminary tests on candidate scintillators for the iMPACT calorimeter were conducted at the CN Van de Graaff 7 MV electrostatic accelerator, at INFN Laboratori Nazionali di Legnaro (LNL), using 3.5 MeV and 5 MeV protons. The main goal of these tests was to characterize the response of a single PVT scintillating finger coupled to a SiPM. The setup, fig. 6 (left), housed in a vacuum chamber, included two BC-420 scintillator fingers, with two different wrapping materials, teflon and aluminum, for comparison. The aluminum solution was later discarded due to its lower reflectivity. In both cases the opening of two dedicated holes in the wrapping, at a distance d of 50 and 150 mm from the SiPM base, was necessary to allow such low energy protons enter the scintillator volume. The setup for this early test was equipped with a provisional read-out electronics, as the design of a dedicated electronics for the iMPACT calorimeter was still in progress. The parameters of the GATE simulation, such as light yield and scintillation time constant, were calibrated using data sets relative to the two different energies and the two proton incident positions.

Nevertheless, the experimental measurements highlighted a non-expected time structure of the light signal, where fast ripples are clearly visible at the output, as shown in

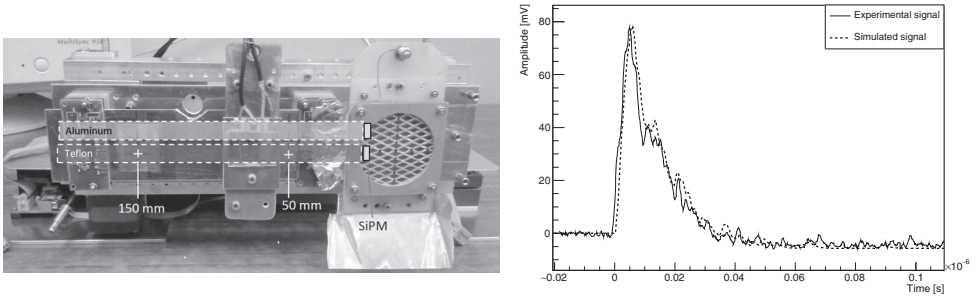

Fig. 6. – Experimental setup used for the test beam at INFN-LNL CN accelerator. Teflon and aluminum wrapped fingers are highlighted (left). Comparison between an experimental and a GATE simulated waveform, in the configuration $E = 5$ MeV and $d = 50$ mm (right).

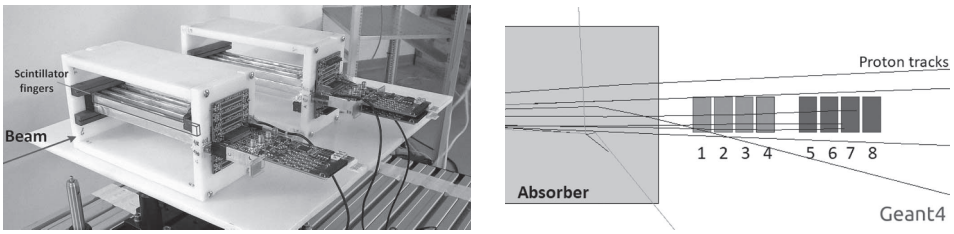

Fig. 7. – Setup used for the test at the INFN-TIFPA APSS proton beam line (left). Setup as modelled in GATE showing the 8 aligned BC-408 PVT fingers after the absorber (right), with superimposed proton tracks.

fig. 6 (right). The simulated analog output signals were able to reproduce the effect, which is due to the high aspect ratio of the finger (20:1) and the statistical nature of the light signal formation in the scintillator, which becomes more apparent for low light yields.

6. – Calorimeter test

A second characterization with proton beam was performed at the experimental line of the Trento Institute for Fundamental Physics and Applications (TIFPA) hosted at APSS, Azienda Provinciale per i Servizi Sanitari, proton therapy facility in Trento [10]. This facility is designed around an IBA Proteus 235 cyclotron, which can accelerate protons at energies between 70 MeV and 228 MeV, and includes two medical treatment rooms. Outside clinical hours, the beam can be redirected towards an experimental room, managed by TIFPA, to address to a wide range of scientific applications.

A multiple-finger layout was studied in this test. The fingers were arranged in two identical units, as shown in fig. 7; each unit included 8 PVT fingers aligned in two rows along the beam direction, together with their full DAQ, SiPM, and read-out electronics. The entire top row included 8 identical BC-408 fingers and 3 mm × 3 mm Hamamatsu S12572-025c SiPM, while the lower row included both BC-420 and BC-408, as well as a different SiPM model (Hamamatsu S12571-015C), for comparison tests. The read-out electronics used during this test was, unlike the provisional one used during the previous test at INFN-LNL, designed specifically for iMPACT. The setup also included a plexiglass absorber to mimic the missing calorimeter layers. The thickness of the absorber was calibrated (about 28 cm) to have the 228 MeV protons stopping inside the fingers. The relative position of the calorimeter modules and the absorber could be modified in order to measure the response to protons in different configurations. In particular, the configuration with the absorber in front of the two modules, which is shown using a GATE representation in fig. 7 (right), allows to observe the proton energy loss profile around the Bragg peak, to study the capability of the iMPACT calorimeter to measure the proton stopping position.

An issue caused by using one single instrumented row of scintillators is that a significant portion of the detected protons scatters out of the PVT volumes, without releasing their entire energy inside the fingers. The complete iMPACT calorimeter, where the total absorbing volume would be large enough to contain also protons deviating from the straight path, would not suffer this issue. A discrimination method has to be applied in order to reject protons scattering out of the fingers and to observe a clear Bragg peak.

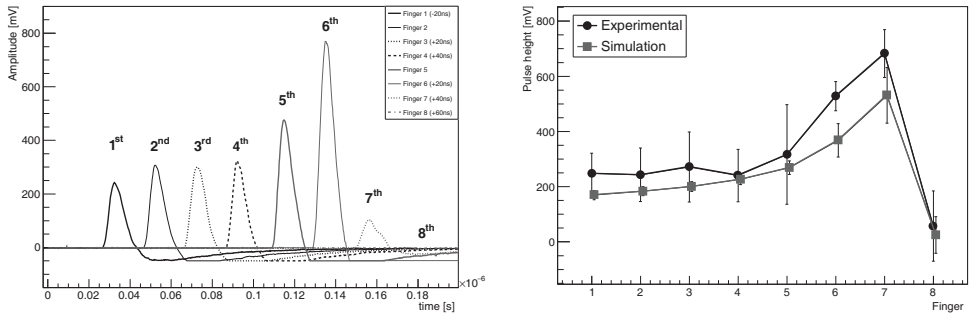

Fig. 8. – Measured signals in the 8 fingers, from the same proton event (left). Signal waveforms are time-shifted for sake of clarity. Average signal amplitude, integrated over multiple events, along the 8 fingers (right), compared for experimental and simulated (slightly shifted for clarity) data.

Experimental data, as well as information from simulated events, show that the 228 MeV proton Bragg peak is shared between the 6th and the 7th finger, therefore a threshold on the sum of their signal amplitudes, $V_6 + V_7$, was defined in order to select protons stopping inside the fingers. A threshold level of $V_6 + V_7 > 1100$ mV was found to efficiently reject spurious events, based on both experimental data and simulation results. The details about the discrimination procedure can be found in [12].

The experimental signals in the 8 consecutive fingers, generated by a single proton event, are shown in fig. 8 (left); the signals are time shifted with respect to each other for the sake of clarity. The signal amplitudes outline the energy loss profile of the proton. The energy loss in the first 4 fingers is almost constant; the energy deposition then increases in the following fingers, reaching the maximum level in the 6th finger. The proton then travels a short distance inside the 7th one and stops; in fact, no signal is registered inside the last (8th) finger. The finger where the proton comes at rest is therefore clearly recognizable; moreover the shape of the Bragg peak is distinguishable.

The average experimental pulse amplitude in each finger, integrated over the events remaining after the application of the threshold on $V_6 + V_7$, is shown in fig. 8 (right). The energy deposition profile is almost constant in the first four fingers (average signal around 250 mV, corresponding to a deposited energy of about 5.5 MeV per finger). The profile presents, as expected, a maximum in the 7th finger, with about 16.5 MeV deposited. The energy deposition profile retrieved from simulated data is also presented in the same plot: the simulated energy profile shares the same behaviour with respect to the experimental data, however, with a smoother trend. The simulated profile presents generally lower values than the experimental one; this is because the simulation was performed using the parameters calibrated with the BC-420 finger version, given the fact that the characterization of the BC-408 used for this test is still ongoing. Therefore, results obtained from experimental and simulated data are to be compared only qualitatively.

Energy spectra from different fingers, with the threshold on $V_6 + V_7$ applied, are presented in fig. 9 for both experimental (left) and simulated (right) data. The 1st and the 3rd finger spectra are, as expected, overlapped, being in the initial region of the energy deposition profile. The 7th finger, where the highest average energy deposition takes place, shows a wider spectrum than the other ones. This clear separation between the finger in which the proton Bragg peak occurs and the previous ones, indicates that

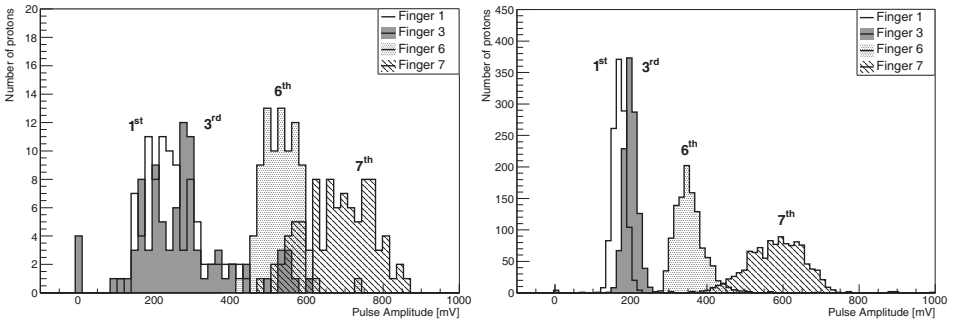

Fig. 9. – Signal amplitude spectrum from 1st, 3rd, 6th and 7th fingers, from experimental (left) and simulated (right) data, with threshold on $V_6 + V_7$.

the concept of an energy range counter is applicable, even with a low sampling precision ADC. The simulated spectra show a comparable behaviour with the experimental one, however the 6th finger spectrum is translated towards lower energies, and farther from the 7th finger spectrum. The simulation, additionally, underestimates the energy distribution spread. The differences between the measurements and the simulation results are likely due to the significant presence of materials in the experimental setup, which was not considered in the simulation; these materials could cause a broadening of the beam dimensions, defocussing, as well as widening and a lowering of its energy distribution. Furthermore, some discrepancies can derive from inaccurate modelling of the absorber dimension, chemical composition and density. Further tests are required in order to fully characterize BC-408 scintillator fingers, parameterizing their light yield as well as energy resolution and time response.

The analysis on the data collected during the test, with the calorimeter modules and the absorber in different configurations, as well as different beam energies, is still ongoing.

7. – Future outlooks: the tracking system response evaluation

A quick demonstrative measurement using the ALPIDE pixel sensor was performed during the INFN-TIFPA beam time, using 70 MeV protons, in order to illustrate the potential of a large area MAPS sensors in imaging applications. A ballpoint pen was taped on the support structure of the ALPIDE, with the tip of the pen placed directly

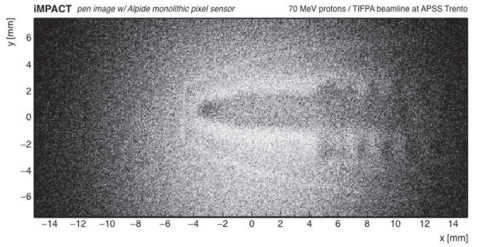

Fig. 10. – Proton radiography of a ballpoint pen tip, as hits on the ALPIDE pixels, for a total of $6 \cdot 10^5$ events. Each point represents a single $28\,\mu$m$\times$ $28\,\mu$m pixel, while the gray scale is indicative of the number of hits, with a lighter color corresponding to a higher number of hits.

in front of the active area of the detector. The hit map of the protons on the sensor, shown in fig. 10, outlines the shape of the internal components of the pen: the spring, the metallic tip and the plastic cap are visible. A darker circle is noticeable at the end of the metallic tip, corresponding to the ballpoint of the pen, which, due to its higher density, projects a darker shadow.

8. – Conclusions

Initial tests on the early prototype of the iMPACT calorimeter have been performed. The success of tests demonstrates that a full calorimeter is indeed feasible, and validates the idea of an hybrid energy range calorimeter as an effective component of a fast and accurate proton tomography scanner. A simulation tool has been also developed to study the behavior of the calorimeter and help choose among different design options. The simulation-based evaluations are compatible with the actual measurements. The simulation code will be further optimized and will play a key role in guiding the full development of the iMPACT calorimeter. The first tests on the ALPIDE with protons illustrate the potential of large area MAPS sensors in imaging applications.

* * *

The iMPACT project is funded by an European Community ERC Consolidator Grant (649031).

REFERENCES

[1] Suit H. *et al.*, *Radiother. Oncol.*, **95** (2010) 3.
[2] Sadrozinski H. F. W. *et al.*, *IEEE Trans. Nucl. Sci.*, **51** (2004) 3.
[3] Bar E. *et al.*, *Med. Phys.*, **44** (2017) 2332.
[4] Schneider U.*et al.*, *Med. Phys.*, **31** (2004) 1046.
[5] Civinini C. *et al.*, *JINST*, **12** (2017) C01034.
[6] Zygmanski P. *et al.*, *Phys. Med. Biol.*, **45** (2000) 511.
[7] Giacometti V., *Modelling and improvement of proton computed tomography*, PhD Thesis, *University of Wollongong* (2016).
[8] Schulte R. *et al.*, *Med. Phys.*, **35** (2008) 4849.
[9] Petterson M. *et al.*, *Proton radiography studies for proton CT*, in *Nuclear Science Symposium Conference Record IEEE*, Vol. **4** (2006).
[10] Tommasino F. *et al.*, *Nucl. Instrum. Methods A*, **869** (2017) 15.
[11] ALICE Collaboration (Mager M. *et al.*), *Nucl. Instrum. Methods A*, **824** (2016) 434.
[12] Baruffaldi F., *Studies for a proton tomography scanner*, Master Degree Thesis, *University of Padova* (2017).
[13] Jan S. *et al.*, *Phys. Med. Biol.*, **49** (2004) 4543.